EPJ Web of Conferences **288**, 04023 (2023) https://doi.org/10.1051/epjconf/202328804023
ANIMMA 2023

Simultaneous inter-calibration of 160 MiMi neutron detectors

Fanny Vitullo[1,*], Vincent Lamirand[1,2], Daniel Godat[1], and Andreas Pautz[1,2]
[1]École polytechnique fédérale de Lausanne (EPFL), CH-1015 Lausanne, Switzerland
[2] Paul Scherrer Institute (PSI), CH-5232, Switzerland

(*) fanny.vitullo@epfl.ch, vincent.lamirand@epfl.ch

***Abstract*—The 160 MiMi neutron detectors of SAFFRON, a 3D full-core mapping system developed at EPFL for the CROCUS zero-power reactor, have been simultaneously inter-calibrated in preparation for their in-core installation. An experimental setup was built to distribute up to 180 MiMi detectors radially at 15 cm around the Pu-Be neutron source of the CARROUSEL facility. An efficient inter-calibration methodology is presented: first, the azimuthal shape of the relative source strength is characterized by rotating 18 MiMi detectors distributed every 20° around the Pu-Be, followed by the simultaneous determination of the relative sensitivity of 160 MiMi detectors, distributed all around the Pu-Be source.**

***Keywords*—Neutron detector, MiMi detector, Inter-calibration, Pu-Be neutron source, CARROUSEL, Relative sensitivity, Source factor, CROCUS.**

I. INTRODUCTION

THE development of a three-dimensional (3D) full-core mapping system, called SAFFRON [1], was initiated in 2020 for its installation in the core of the CROCUS zero-power research reactor [2], [3] operated at the Ecole Polytechnique de Lausanne (EPFL), Lausanne, Switzerland. SAFFRON consists of 149 miniature and minimalistic (MiMi) neutron detectors [4], [5] distributed at different radial and axial inter-pin locations of the CROCUS core (plus 11 mobile MiMi detectors), the detectors' supporting structure, and custom digital readout electronics. SAFFRON, with its large number of neutron detectors distributed in between fuel rods and covering the entire core volume, targets the investigation of space-dependent neutronics phenomena in CROCUS and enables the online measurement of thermal neutron flux maps in both a static and time-dependent fashion.

Among SAFFRON objectives, the experimental reconstruction of the 3D thermal neutron flux shape of the CROCUS core is envisaged for future comparison with high-fidelity reactor physics codes results [6]. However, each of the SAFFRON detectors is a unique hand-made instrument, with peculiar counting capabilities, exposed to a different thermal neutron flux dictated by its core location. For this reason, the knowledge of the relative sensitivity ε between MiMi neutron detectors is essential to rescale their count rate readings and obtain a detector-independent shape of the CROCUS thermal flux map.

In this work, the 160 MiMi neutron detectors of SAFFRON are inter-calibrated prior to their in-core installation with the Pu-Be source installed in the CARROUSEL facility, operated at EPFL. The innovative inter-calibration methodology proposed in this work aims at retrieving efficiently and in a short time the relative sensitivities between such a large number of MiMi detectors while reducing experimental uncertainties.

II. MIMI NEUTRON DETECTORS

The MiMi neutron detectors [4], [5] have been developed at EPFL since 2018 targeting a variety of zero-power reactor applications ranging from the investigation of localized neutronics phenomena in CROCUS, i.e., azimuthal flux dependencies [7] and lateral fuel rod displacements [8], [9], to their application to 3D full-core mapping systems such as SAFFRON [1].

The MiMi technology features an inorganic ZnS(Ag):^{6}LiF scintillator screen [10] positioned at the front-end of a plastic optical fiber [11] (see Fig. 1) transporting the scintillation light from the detector's active volume to a silicon photomultiplier (SiPM) [12] to count thermal neutron interactions after proper signal processing with either analog or digital readout electronics.

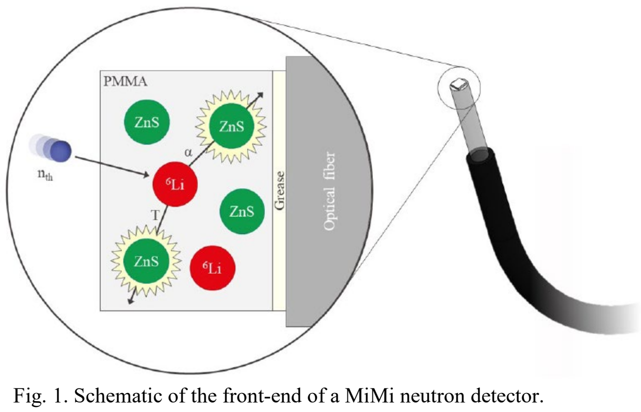

Fig. 1. Schematic of the front-end of a MiMi neutron detector.

A. *Upgrade to SAFFRON version*

The latest version of MiMi neutron detectors used in the SAFFRON system is composed of a 0.225-mm thick ZnS(Ag):^{6}LiF screen cut into 0.66×0.66 mm squares using a precise wire-cutting technique. The screen is positioned at the tip of the sanded and uncovered tip of the 1-mm diameter optical fiber PMMA core (2.2 mm of total external diameter) with a layer of optical grease in between the two. The fiber tip is covered with an aluminum cap having the same external diameter as the optical fiber. The cap is glued to the optical fiber with an epoxydic adhesive (Araldite), used due to its excellent resistance in the water, fast setting, and good transparency to prevent both unwanted movements or loss of the screen in the CROCUS core.

A crucial upgrade for the extension of the applicability of MiMi detectors to full-core mapping systems was the transition from an analog readout system to a custom-made six-module multi-channel processing electronics system, coupled with FPGA-based digital readout [1]. The combination of the two systems allows the simultaneous processing and acquisition of up to 160 MiMi detector signals.

B. Detector sensitivity

Each individual MiMi neutron detector is unique, as it was manufactured first-hand and in series directly at EPFL. In fact, different MiMi detectors measuring in the same neutron field, in terms of neutron flux level and spectrum, show variations in their thermal neutron counting capabilities. These disparities can arise from several factors:

- *Different amounts of ^{6}Li converter*: inhomogeneities in the mixing of ^{6}LiF and ZnS in the screen, or slight variations of screen thickness or size (after cutting) may affect the neutron count rate;
- *Photon yield variations*: variations in the ZnS concentration, misalignments in the positioning of the scintillator screen at the tip of the optical fiber, and infiltrations of filtering materials as glue or dirt may reduce the light collection efficiency causing detector spectrum shifts and, consequently neutron count rate variations;
- *Efficiency of processing electronics*: the SiPM photon detection efficiency and the capabilities of the processing electronics to transform SiPM signals into photon counts might differ due to manufacturing. In this work, each scintillator screen is always paired with its own fixed SiPM and processing electronic channel, and no cross-connections are performed.

The quantity describing the counting capabilities of a single neutron detector is the intrinsic counting efficiency ϵ, or sensitivity, which relates the detector output with the amount of radiation incident on the active detector volume [13]. Instead, the relative sensitivity $\varepsilon_{i,j}$ between two detectors i and j is defined as:

$$\varepsilon_{i,j} = \frac{\epsilon_i}{\epsilon_j} \qquad \text{Eq. 1}$$

and is a characteristic parameter of the detector's duo. $\varepsilon_{i,j}$ can be considered independent of the experimental setup and the irradiation conditions in which it is measured, as long as the two detectors experience a similar neutron spectrum and they will be further used in neutron fields with a similar spectrum. In the particular case of the MiMi neutron detectors, it is also important to maintain the same connection between the ZnS(Ag):^{6}LiF screen and its SiPM to obtain reproducible values of $\varepsilon_{i,j}$.

III. The CARROUSEL facility

CARROUSEL is a nuclear facility operated at EPFL and consisting of a Pu-Be neutron source installed at the center of a cylindrical stainless steel (SS) tank filled with water. Neutrons are produced via the (α, n) reaction between an α particle generated by the decay of ^{239}Pu and a ^{9}Be nucleus as:

$$^{9}_{4}Be + \alpha \rightarrow {}^{12}_{6}C^* + n \rightarrow {}^{12}_{6}C + n + \gamma \qquad \text{Eq. 2}$$

The Pu-Be source of CARROUSEL emits 8.9 × 10^6 neutrons/s [14] with an energy spectrum of 3.5 MeV average and 10.6 MeV maximum energy. Although different shapes of the neutron emission energy spectrum of Pu-Be sources are available in literature [15], [16], the spectrum of the CARROUSEL source is not characterized. However, it was shown that the neutron spectrum becomes fully thermal after 10 cm of distance from the source center [17]. In addition, the 4.4-MeVgamma rays originating from the de-excitation of ${}^{12}_{6}C^*$, make CARROUSEL a mixed neutron-gamma field facility.

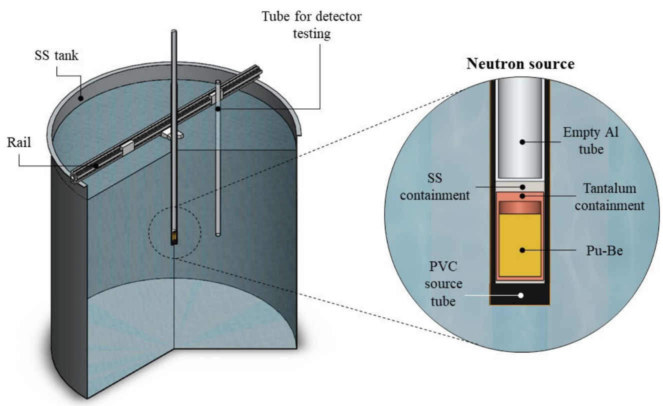

Fig. 2. Schematic of the CARROUSEL facility operated at EPFL.

As shown in Fig. 2, the Pu-Be source has a cylindrical shape, with a double-wall container made of tantalum and welded stainless steel. The source is connected to an aluminum tube for facilitating a convenient and safe handling. On occurrence, the source, along with the handling tube, is inserted into a Polyvinyl chloride (PVC) tube of 40 mm of internal diameter and 3.2 mm thickness positioned in the central vertical axis of the water tank. The PVC tube, designed so that the Pu-Be source is located at mid-height of the water tank, is held in position by being attached to a horizontal rail installed above the tank. The same rail is also used to install and move plastic measurement tubes where different neutron detectors can are installed at will for teaching and research purposes. Finally, the water tank is filled with industrial water at approximately 12 ºC, and gradually reaching thermal equilibrium with the controlled area's temperature of 20 °C.

IV. INTER-CALIBRATION METHODOLOGY

The inter-calibration procedure presented in this work aims at finding the relative sensitivity $\varepsilon_{i,j}$ between MiMi detectors in a well-known thermal neutron field in order to successively re-apply those factors for rescaling experimental flux shape measurements in CROCUS as:

$$\frac{\phi_{th,i}}{\phi_{th,j}} \propto \frac{CR_i}{CR_j} \cdot \frac{1}{\varepsilon_{i,j}} \qquad \text{Eq. 3}$$

where $\phi_{th,i}$ and $\phi_{th,j}$ are the thermal neutron fluxes in two core locations, and CR_i and CR_j are the count rates of the MiMi detectors at the corresponding locations.

The CARROUSEL facility was selected to perform the MiMi detectors' inter-calibration, as readily available at EPFL. The classic neutron detector calibration methodology used in CARROUSEL consists in measuring the relative sensitivity between two detectors by positioning them alternatively in the same measuring tube, located at a fixed radial distance from the source, and compare their count rate in constant irradiation conditions. This method would allow to retrieve relative efficiencies independently from possible Pu-Be source anisotropies. However, due to the large number of detectors to be inter-calibrated for the SAFFRON system, such procedure would be time-consuming and cumbersome, resulting in larger experimental uncertainties. Therefore, an innovative methodology was developed ad-hoc to simultaneously inter-calibrate up to 160 MiMi neutron detectors in the CARROUSEL facility. This methodology includes two steps: first, the experimental characterization of the Pu-Be azimuthal source factor, and then the simultaneous inter-calibration of 160 MiMi detectors.

A. *Mathematical formulation*

Considering a generic neutron source located in the center of a non-multiplying media, the intrinsic sensitivity ϵ of a neutron detector, positioned at a radial distance r from the source with an azimuthal angle θ and a polar angle φ, within a neutron energy spectrum χ, can be defined as:

$$\epsilon = \frac{CR(m,g,\chi,r,\theta,\varphi)}{S(g,\chi,r,\theta,\varphi)} \qquad \text{Eq. 4}$$

where:

- $CR(m,g,\chi,r,\theta,\varphi)$ is the detector's count rate. It depends on the detector's properties, i.e., material composition m and detector geometry g, the neutron energy spectrum χ, and the detector position (r,θ,φ);
- $S(g,\chi,r,\theta,\varphi)$ is the source factor and represents the number of neutrons with a χ spectrum incident on the detector's geometry g when placed at (r,θ,φ) coordinates.

If the radial distance r and the polar angle φ at which the detector is positioned with respect to the point source are fixed, and the neutron spectrum is constant at different azimuthal coordinates θ, Eq. 4 can be simplified as:

$$\epsilon = \frac{CR(m,g,\theta)}{S(g,\theta)} \qquad \text{Eq. 5}$$

The relative sensitivity $\varepsilon_{i,j}$ between two neutron detectors i and j with similar geometrical properties $g_i \approx g_j$, but different material composition $m_i \neq m_j$, positioned respectively at the azimuthal angles θ_i and θ_j is defined as:

$$\varepsilon_{i,j} = \frac{\epsilon_i}{\epsilon_j} = \frac{CR_{i,\theta_i}}{CR_{j,\theta_j}} \cdot \frac{S_{\theta_j}}{S_{\theta_i}} \qquad \text{Eq. 6}$$

In case the two detectors are positioned alternatively at the same azimuthal position $\theta_i = \theta_j = \bar{\theta}$, or if the source factor shows an isotropic azimuthal profile, the relative sensitivity $\varepsilon_{i,j}$ between two detectors becomes simply the ratio of their count rates:

$$\varepsilon_{i,j} = \frac{CR_i}{CR_j} \qquad \text{Eq. 7}$$

On the contrary, if the azimuthal profile of the neutron field $S(\theta)$ is unknown, the prior estimation of the relative source factor $s_{\theta_i,\theta_j} = S_{\theta_j}/S_{\theta_i}$ is essential to derive the relative sensitivity between geometrically similar detectors, as per Eq. 6, without having to perform their inter-calibration by positioning them one-by-one in constant irradiation conditions $S(\bar{\chi},\bar{r},\bar{\theta},\bar{\varphi})$.

B. *Source factor characterization*

The source factor characterization in the CARROUSEL facility consists in finding the $S(\theta)$ profile with respect to a reference azimuthal position, at fixed radial $\bar{r}$ and polar $\bar{\varphi}$ coordinates, and in a constant neutron spectrum $\bar{\chi}$.

1) *Simple case methodology*

Two detectors of similar geometries, called detector 0 and detector 1, are located respectively at the azimuthal positions α and β, and both are at the same fixed $\bar{r}$ and $\bar{\varphi}$ around a neutron source. The count rates measured by the two detectors, having similar geometrical properties, are:

$$\begin{aligned} CR_{0,\alpha} &= \epsilon_0 \cdot S_\alpha \\ CR_{1,\beta} &= \epsilon_1 \cdot S_\beta \end{aligned} \qquad \text{Eq. 8}$$

If the azimuthal position of the two detectors is switched, the successive measurement yields to:

$$\begin{aligned} CR_{0,\beta} &= \epsilon_0 \cdot S_\beta \\ CR_{1,\alpha} &= \epsilon_1 \cdot S_\alpha \end{aligned} \qquad \text{Eq. 9}$$

By summing the two independent experimental output obtained with different detectors at the same azimuthal coordinate, the following quantities are obtained:

$$\begin{aligned} CR_{0,\alpha} + CR_{1,\alpha} &= (\epsilon_0 + \epsilon_1) \cdot S_\alpha \\ CR_{0,\beta} + CR_{1,\beta} &= (\epsilon_0 + \epsilon_1) \cdot S_\beta \end{aligned} \rightarrow \frac{S_\alpha}{S_\beta} \quad \text{Eq. 10}$$

The ratio between the right-hand terms of Eq. 10 leads to the estimation of the relative source factor $s_{\alpha,\beta} = S_\alpha / S_\beta$. In a similar way, the ratio between the sum of count rates measured at different azimuthal angles with the same detector returns the relative detector efficiency $\varepsilon_{0,1} = \epsilon_0 / \epsilon_1$:

$$\begin{aligned} CR_{0,\alpha} + CR_{0,\beta} &= \epsilon_0 \cdot (S_\alpha + S_\beta) \\ CR_{1,\alpha} + CR_{1,\beta} &= \epsilon_1 \cdot (S_\alpha + S_\beta) \end{aligned} \rightarrow \frac{\epsilon_0}{\epsilon_1} \quad \text{Eq. 11}$$

The strength of this methodology lies in the possibility to assess at the same time both the relative source term and the relative detector efficiency, independently from each other. In this simple case with two detectors, only two experimental measurements are required to obtain independent relative parameters. However, if the number of detectors to be inter-calibrated becomes large, the number of independent measurements required grows linearly, leading once again to a cumbersome procedure. For instance, 160 measurements would be required to perform a full inter-calibration of 160 MiMi neutron detectors with this approach. As a result, this methodology is employed in this work solely with the intent of reconstructing the source factor's shape in CARROUSEL by using a limited number of MiMi detectors.

2) Extension to 18 detectors

The simple methodology described in the previous paragraph was extended to the use of 18 MiMi neutron detectors evenly spaced around the CARROUSEL Pu-Be source. The 18 MiMi detectors, assumed to have a comparable active volume's geometry, are positioned at 15 cm of radial distance from the Pu-Be neutron source of CARROUSEL with an azimuthal spacing of 20 degrees and at the same level of the source mid-height, giving a zero polar coordinate. The radial distance of 15 cm, considerably larger than the neutron slowing-down length of Pu-Be neutrons in water, was chosen to ensure that the scintillator screens are in a thermal neutron spectrum. By re-positioning each detector at each azimuthal position, for a total of 18 measurements, it becomes possible to delineate the relative source term profile $S(\theta)$ with respect to the zero-angle reference position with a 20 degrees resolution. Such azimuthal resolution was deemed appropriate to find a global shape of the source term around the neutron source making use of the number of MiMi neutron detectors available at the time of measurement. A visual illustration of the method extended to 18 detectors is shown in Fig. 3.

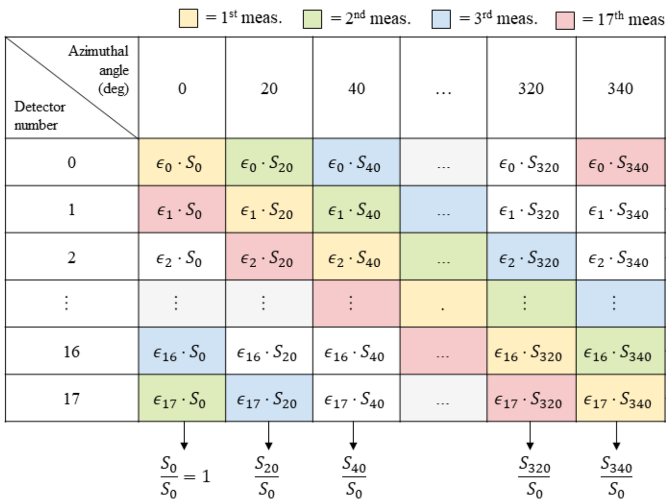

Fig. 3. Visual illustration of the source factor characterization methodology performed in CARROUSEL with 18 MiMi neutron detectors.

C. Relative sensitivity measurement with 160 detectors

Knowledgeable of the relative source factor of the Pu-Be source of CARROUSEL, Eq. 6 is used to rescale the ratio of the count rates between MiMi detectors at different azimuthal positions, but distributed at 15 cm around the Pu-Be source of CARROUSEL with a 2 degrees resolution. In this way, the relative detector efficiencies $\varepsilon_{i,j}$ of 160 MiMi detectors are simultaneously estimated.

V. EXPERIMENTAL SETUP

The MiMi detectors' positioning around the neutron source is performed with a dedicated plastic structure designed and built at EPFL for testing and inter-calibrating all 160 MiMi detectors of SAFFRON. The structure, shown in red in Fig. 4 for visualization purposes, consists of two black POM-C disks of 30.7 cm diameter and 3 cm thickness. The disks, inserted around the CARROUSEL source tube, are held together by three vertical plastic rods dimensioned to position the detectors' active volume at the source mid-level. At the same time, the rods force the upper and lower disk to rotate in solidarity around the source tube. The lower POM-C disk is machined with 180 blind holes of 2.3 mm diameter and 2.2 cm depth, distributed every 2 degrees at 15 cm from the disk center. Each blind hole can accommodate one of the MiMi detectors, safely held in position by a rubber O-ring through a later aperture, as visible in Fig. 4.

A. Setup for source factor characterization

For the source factor characterization experiment, the 18 detectors are positioned one every five holes to respect the desired 20 degrees of spacing. The upper POM-C disk serves as a reference for the azimuthal position of the lower disk. The 36 through holes of 5 mm diameter distributed every 10 degrees around the upper disk define the unit of a rotational step that the structure can perform. A plastic piece attached to the rail running over CARROUSEL allows for the precise selection of the azimuthal coordinate via the insertion of a metallic pin bounding the piece itself and the upper disk through one of its holes. At the initial conditions, the reference MiMi detector is positioned in correspondence with the piece fixating the rotation, oriented towards the west and defining the 0° azimuthal position. The rest of the detectors are distributed counter-clockwise in the lower POM-C disk.

The front-end of each of the 18 MiMi detectors is inserted in the lower disk and is connected via the optical fiber to its own counting channel, composed of a SiPM and a processing board, both part of a multi-channel stand-alone module developed at EPFL for the SAFFRON experiment [1]. In this particular case, the processing channels from ch.65 to ch.82 of module D are used to process the scintillation light. Module D is stored, together with the other five operational modules, in the Memmert IPP750eco incubator [18], kept at a stable temperature of 20 ± 0.1 °C to guarantee stable SiPM photon counting efficiency. SiPMs are operated with a high voltage of 56.66 V, and the conversion of the SiPM output into photon counting is performed with a threshold of 1 V. The photon counting is digitally processed by the CAEN V2495 FPGA [19] with a proprietary firmware based on moving sum differentiation (MSD) algorithm [20]. The resulting thermal neutron counting per channel is sent to the acquisition computer via the CAEN V1718 VME bus [21].

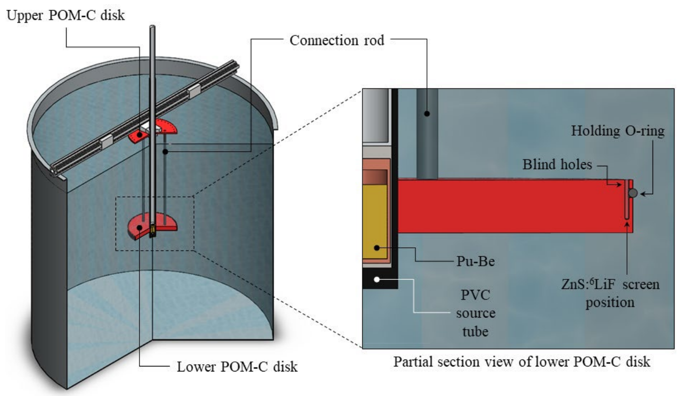

Fig. 4. Experimental setup in CARROUSEL for inter-calibration procedure.

The holding structure is installed and equipped with the 18 MiMi detectors while the water tank of CARROUSEL is empty and the Pu-Be source is not present in the tube. After the installation, the tank is filled with industrial water flowing at around 12 °C of temperature. Three heaters are installed on the side of the water in order to speed up the attainment of the thermal equilibrium between the industrial water and the controlled area environment, kept constant at around 20°C. Once the water equilibrium temperature is reached, the series of 18 measurements by rotation of the structure is started. Each counting measurement is named as the azimuthal position of det. #0. The selection of the azimuthal position is optimized to obtain preliminary results and, for this reason, it is not performed following the increase of the azimuthal angle with respect to the initial position (corresponding to the reference detector at position 0°) linearly. All the measurements are performed continuously, with only interruptions of a few minutes to manually rotate the holding structure and the 18 MiMi detectors together with it. In this way, potential drift due to external conditions, such as the water temperature, can be taken into account and quantified. The measuring time at each azimuthal position was chosen to have an uncertainty of at least 0.5% on the measured count rate of each MiMi detector at every azimuthal position. The minimum measuring time at each azimuthal position is about 2 hours, while five sub-measurements of approximately 20 minutes are automatically run by the digital readout. Longer measurements – performed with continuous sub measurements during nights and weekends – contribute to lowering the final uncertainty of the source factor profile.

B. Setup for the inter-calibration

The CARROUSEL tank was then emptied after properly storing the Pu-Be source, and the same setup was equipped with 160 MiMi neutron detectors in preparation of the measurement to simultaneously inter-calibrate them. The 160 MiMi detectors are labeled with numbers going from det.#0 to det.#159. The detectors from #0 to #155 are installed in the lower POM-C disk occupying the azimuthal positions from 0° to 310° with a 2° spacing. The remaining 4 MiMi detectors are spread in the last 50° to cover the entire range of azimuthal coordinates. Hence, these detectors are positioned every 10° and are accompanied by two small fictive detectors in the neighboring azimuthal positions to reproduce potential self-shielding effects between detectors as in the other 156.

The five stand-alone processing modules A, B, D, E, and F are installed inside the Memmert IPP750 eco incubator set at 20 ± 0.1 °C, together with the digital read-out electronics composed of the FPGA and the VME bus from CAEN. Each optical fiber is connected to one of the counting channels of the multi-channel processing electronics. The connection follows the detector numbering in a way that det.#0 is connected to ch.0, det. #1 is connected to ch.1, and so on. The same connection between the MiMi active volume and its processing channels must be maintained when installing the detectors in-core with the SAFFRON system. All the MiMi detectors are inter-calibrated with respect to the det.#0, positioned in the reference 0° azimuthal position of CARROUSEL. The duration of the counting experiment is dictated by the need for low statistical uncertainties in the counting. A total acquisition time above 40h was estimated sufficient to obtain uncertainties in the order of 0.1% on the single detector count rate of approximately 7.5 cps. The 42-h acquisition is divided into consecutive automatic sub-measurements of approximately 15 minutes each with the intent to observe potential trends over time and split the result data files.

At the starting time, the heaters installed in CARROUSEL are left intentionally powered after already two hours of functioning to observe if there are effects related to the water temperature increase. They are tuned off after about four hours, and the water is mixed at the same time, reaching the temperature of 21°C at approximately the mid-height level of the tank water. The data acquisition from the next 16 hours is discarded to let the CARROUSEL tank reach equilibrium with the environment, followed by the 42-h acquisition.

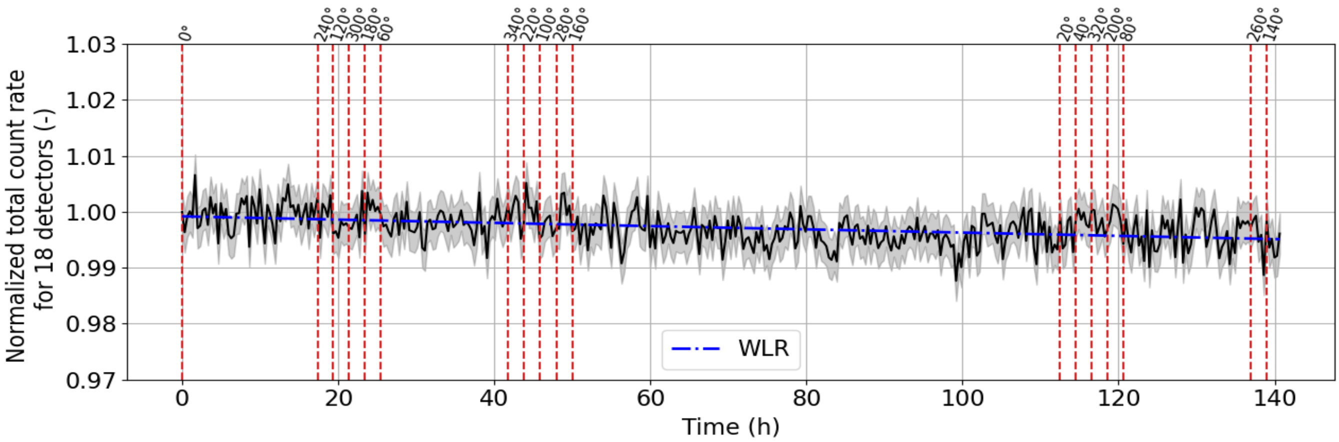

Fig. 6. Normalized total count rate for the 18 MiMi detectors used for source characterization as a function of the measuring time in CARROUSEL. Vertical red lines represent a change in the detector position, indicated as the azimuthal coordinate of det. #0. The trend from linear regression of data is in blue.

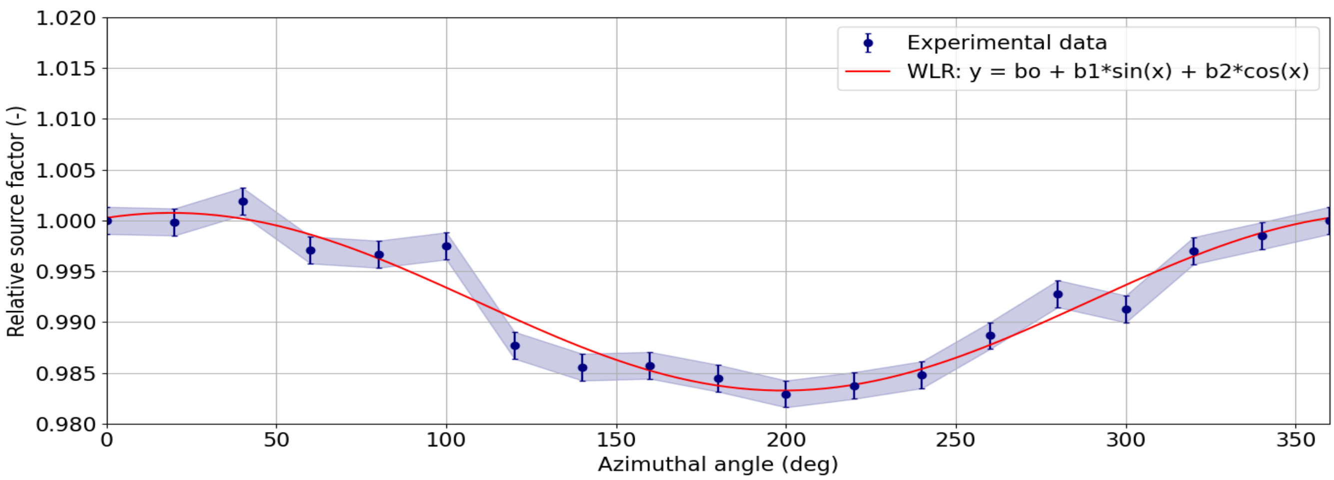

Fig. 5. Relative source factor profile at 15 cm from the Pu-Be source in CARROUSEL.

VI. Inter-calibration results

A. Relative source strength

The trend of the total count rate for the 18 MiMi detectors during the whole measuring time is shown in Fig. 5, normalized to its value at the first 20-min sub-measurement. Observing the trend of total count rate instead of those of single detectors allows to reduce the magnitude of the statistical counting uncertainties. The normalized total count rate for the ensemble of 18 MiMi detectors presents a slight negative drift. The drift magnitude was estimated with a weighted linear regression (WLR). A t-test for the regression slope was performed, resulting in the conclusion that a statistically significant drift is present in the total count rate of 18 MiMi detectors. Such drift causes a reduction of the total count rate of -0.48 ± 0.05 % at the end of the measuring time with respect to the initial conditions. The causes of this drift are yet to be investigated and clarified, although it is possible that the drift is linked to an observed drift in the CARROUSEL water temperature from 19°C to 22°C between the beginning and the end of the measurement. It was estimated that such a temperature variation has a negligible impact on the moderation properties of water and plastic. Hence, the suspect is that a water temperature variation is influencing either the optical properties of the ZnS(Ag):^{6}LiF screen, increasing its opacity, thus reducing the amount of photons emerging from the screen and transported to the SiPM, or respective optical indices between screen, optical grease and fiber. Nevertheless, it was estimated that a correction of the experimental data for the drift, under the assumption that it is constant and equal among all 18 detectors, induces variations in the order of 0.001% in the shape of the source factor and can therefore be neglected.

The source factor shape for the uncorrected data is presented in Fig. 6. The uncertainty on the relative source factor is in the order of 0.14%. A reduction of -1.5% in the source factor shape at 15 cm from the source corresponding to the 200 degrees azimuthal angle is visible in Fig. 6. Assuming that the detectors were perfectly positioned and aligned, which was continuously verified along setup and testing, the causes for such reduction could be:

- An anisotropy of the Pu-Be source of CARROUSEL, attenuated by the water volume and the lower disk plastic at 15 cm;
- A miss-centering towards the azimuthal direction of 200° of the Pu-Be source in its dedicated tube.

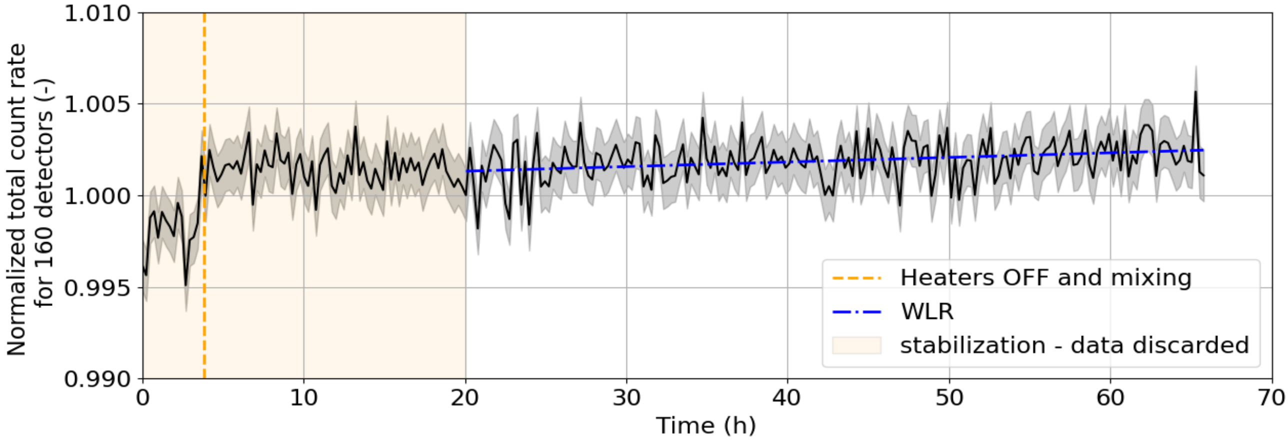

Fig. 8. Normalized total count rate for 160 MiMi detectors as a function of the acquisition time during inter-calibration.

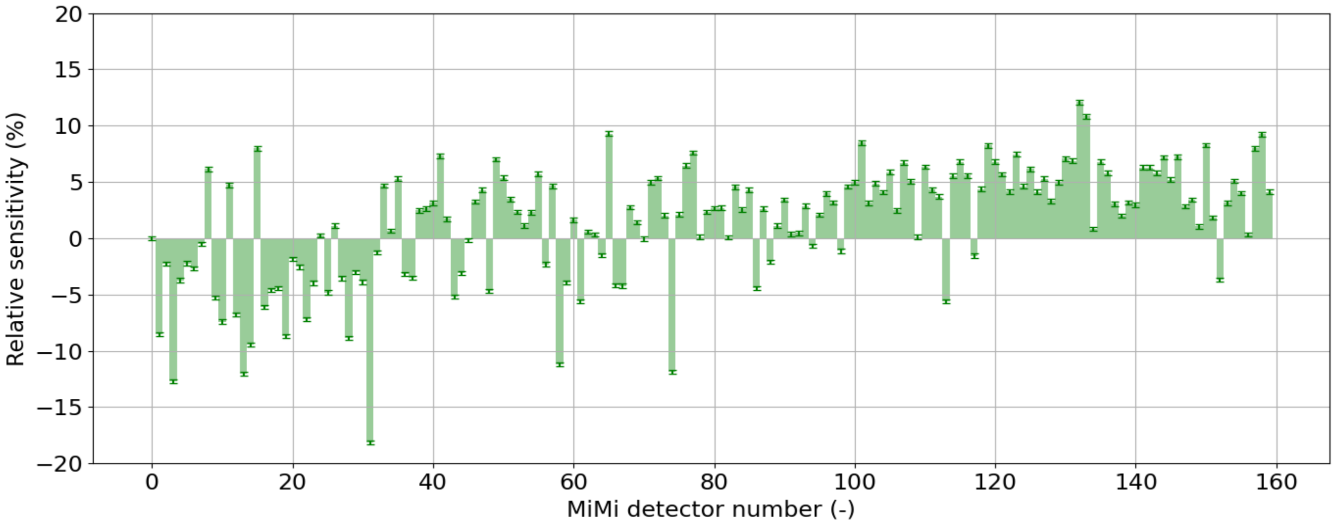

Fig. 7. Relative sensitivity for 160 MiMi detectors with respect to det. #0. The values shown are for data corrected by the total count rate drift.

Considering the known difficulties in the manufacturing and characterization of Pu-Be sources, and the low mechanical play between source and tube (mm-range), as well as its probably low incidence, we rather favor the first option as an explanation.

The experimental data are fitted with a sine function having a 2π period, linearized as $y = b_0 + b_1 \cdot \sin(x) + b_2 \cdot \cos(x)$ with the regression parameters given in Table I.

TABLE I
WLR PARAMETERS FOR THE LINEARIZED SINE FUNCTION DESCRIBING THE RELATIVE SOURCE FACTOR IN THE CARROUSEL FACILITY.

Regression parameter	*Value*	*Standard error*
b_0	0.992	< 0.001
b_1	0.003	0.001
b_2	0.008	0.001

B. Relative MiMi detectors sensitivities

The trend in time of the total number of counts acquired during the 42-h inter-calibration measurement is reported in Fig. 7. At the time of water mixing, an increase in the total count rate in the order of 1% is clearly visible. This represents an ulterior proof of the influence of the water temperature on the detector counting capabilities. However, further investigations are necessary to conclude how the direction of the change is caused by an increase in the water temperature. After the stabilization time, the normalized total count rate for the 160 MiMi detectors shows as well a slight positive and statistically significant drift.

The count rate for each MiMi neutron detector acquired over the entire acquisition time is first corrected by the drift, under the assumption that it is constant and equal for all the detectors, and then normalized by the same value for the det. #0 positioned at the 0° reference position of CARROUSEL. Following Eq. 6, each normalized count rate is divided by the value of the linearized sine function with the parameters in Tab. 1, representing the relative source factor at 15 cm in CARROUSEL. The final values obtained are the relative sensitivities of the 160 MiMi neutron detectors with respect to det.#0. The maximum uncertainty of 0.13% measured on the relative source factor azimuthal points is added to the final computation of uncertainties for conservative purposes. The relative detector sensitivities $\varepsilon_{i,0}$ for corrected data are shown in Fig. 8.

The 160 MiMi neutron detectors show differences in the relative sensitivity between -18.2 ± 0.2 % and +12.1 ± 0.2%. The average uncertainty is 0.2%. The difference between corrected and uncorrected data is calculated to be within the final uncertainty, including the uncertainty of the source factor, and indicates that the total count rate drift can be neglected in the estimation of the relative sensitivities.

VII. CONCLUSIONS

A methodology to simultaneously inter-calibrate 160 MiMi neutron detectors, built for being installed in the CROCUS zero-power reactor as part of the SAFFRON 3D full-core mapping system, was developed in this work. The proposed methodology was performed in the CARROUSEL facility and consists in two-steps: first the relative azimuthal source factor of the Pu-Be source was experimentally estimated with 18 MiMi neutron detectors, and successively the relative sensitivity of 160 MiMi detectors was measured by installing them all at 15 cm around the Pu-Be source. The advantages of this procedure are a shortening of the measuring time and a reduction of the experimental uncertainties. The experimental results highlighted an anisotropy of -1.5% in the shape of the Pu-Be source factor at 15 cm from the source, while the MiMi detectors' relative sensitivities showed variations between -18.2 ± 0.2 % and +12.1 ± 0.2% with respect to the reference detectors. Such variations in the relative sensitivity might be caused by differences in the amount of sensitive material, in the detector mounting, and in the dedicated processing electronics. The obtained relative sensitivities will then be used to re-scale the count rates of the same MiMi detectors while installed in CROCUS as part of the SAFFRON system, and measure the absolute 3D shape of the thermal neutron flux map in CROCUS.

REFERENCES

[1] F. Vitullo *et al.*, "Design of a 150-miniature detectors 3D core-mapping system for the CROCUS reactor," *EPJ Web Conf.*, vol. 253, 2021.

[2] Nuclear Energy Agency (NEA), "IRPhE Handbook 2020." International Reactor Physics Evaluation Project Handbook (database), 2020.

[3] V. Lamirand, "Installation nucléaire CROCUS - Rapport de sécurité," Techical report RT-100-104-17-48, 2017.

[4] F. Vitullo *et al.*, "Developing and testing a miniature fiber-coupled scintillator for in-core neutron counting in CROCUS," in *EPJ Web Conferences*, 2020.

[5] F. Vitullo *et al.*, "A mm^3 Fiber-Coupled Scintillator for In-Core Thermal Neutron Detection in CROCUS," *IEEE Trans. Nucl. Sci.*, vol. 67, no. 4, pp. 625–635, Apr. 2020.

[6] F. Vitullo, "Miniature and Minimalistic Neutron Detectors for Online High-Resolution Experiments in the Zero-Power Reactor CROCUS," Ph.D. thesis TH9492, École polytechnique fédérale de Lausanne (EPFL), Lausanne, 2022. [Online]. Available: https://infoscience.epfl.ch/record/296483?ln=en

[7] F. Vitullo, V. Lamirand, P. Frajtag, G. Perret, and A. Pautz, "Highly localized azimuthal measurements in the CROCUS reactor towards the validation of high-fidelity neutronics codes," in *EPJ Web of Conferences*, 2021, p. 08014.

[8] F. Vitullo *et al.*, "Millimetric fuel rod displacements: an experimental study of the impact on local thermal neutron flux in the CROCUS reactor," in Proceedings of PHYSOR2022, Pittsburgh, PA, USA, 2022.

[9] V. Lamirand *et al.*, "Local and high distance neutron and gamma measurements of fuel rods oscillation experiments," *EPJ Web Conf.*, vol. 253, p. 04024, 2021.

[10] Scintacor, "Neutron screens," 2020. [Online]. Available: https://scintacor.com/wp-content/uploads/2015/09/Datasheet-Neutron-Screens-High-Res.pdf

[11] Mitsubishi Chemical Co., "ESKA optical fibers." https://www.pofeska.com/pofeskae/product/02/index.html

[12] Hamamatsu Photonics K.K., "MPPC S13360 sereis datasheet." 2016. [Online]. Available: https://www.hamamatsu.com/content/dam/hamamatsu-photonics/sites/documents/99_SALES_LIBRARY/ssd/s13360_series_kapd1052e.pdf

[13] G. F. Knoll, *Radiation detection and measurement*, 4th ed. Hoboken, N.J: John Wiley, 2010.

[14] NUMEC-USA, "Shipping document Pu-Be source." 1961.

[15] L. Stewart, "Neutron Spectrum and Absolute Yield of a Plutonium-Beryllium Source," *Phys. Rev.*, vol. 98, no. 3, pp. 740–743, May 1955.

[16] M. E. Anderson and W. H. Bond, "Neutron spectrum of a plutonium-beryllium source," *Nucl. Phys.*, vol. 43, pp. 330–338, May 1963.

[17] E. L. Brunetto, "Validation of the Serpent 2 model for the CARROUSEL facility," École polytechnique fédérale de Lausanne (EPFL), Semester project, 2020.

[18] Memmert Gmbh, "DS_Memmert Peltier-cooled incubator IPP750eco." [Online]. Available: https://www.memmert.com/products/incubators/peltier-cooled-incubator/IPP750eco/

[19] CAEN, "V2495/VX2495 VME Programmable Logic Unit." 2019.

[20] J.-B. Mosset *et al.*, "A 16-ch module for thermal neutron detection using ZnS:6LiF scintillator with embedded WLS fibers coupled to SiPMs and its dedicated readout electronics," *Nucl. Instrum. Methods Phys. Res. Sect. Accel. Spectrometers Detect. Assoc. Equip.*, vol. 845, pp. 494–498, Feb. 2017.

[21] CAEN, "V1718/VX1718 - VME - USB 2.0 Bridges." 2020.